

Strength-based Design Analysis of a Para-Plow Tillage Tool

H. Kursat CELIK^{1*}, Nuri CAGLAYAN², Mehmet TOPAKCI¹,
Allan E. W. RENNIE³, Ibrahim AKINCI¹

^{1,*}Dept. of Agricultural Machinery and Technology Engineering, Faculty of Agriculture, Akdeniz University, Turkey

²Dept. of Mechatronics Engineering, Faculty of Engineering, Akdeniz University, Turkey

³Engineering Dept., Lancaster University, United Kingdom

Corresponding author	: Dr H. Kursat CELIK
e-mail	: hkcelik@akdeniz.edu.tr
Tel	: +90 242 310 65 70
Fax	: +90 242 227 45 64
Address	: Department of Agricultural Machinery & Technology Engineering, Faculty of Agriculture, Akdeniz University, 07070, Antalya, Turkey

Abstract

In this research, experimental field tests and an advanced computer aided design and engineering (CAD and CAE) based application algorithm was developed and tested. The algorithm was put into practice through a case study on the strength-based structural design analysis of a Para-Plow tillage tool. Para-Plow is an effective tractor attached tillage tool utilised as an alternative to the conventional deep tillage tools used in agricultural tillage operations. During heavy tillage operations, the Para-Plow experiences highly dynamic soil reaction forces which may cause undesired deformations and functional failures on its structural elements. Here, prediction of the deformation behaviour of the tool structure during tillage operation in order to describe optimum structural design parameters for the tool elements and produce a functionally durable tool become an important issue. In the field experiments, draft force and strain-gauge based measurements on the tool were carried out simultaneously. Subsequently, Finite Element Method based stress analysis (FEA) were employed in order to simulate deformation behaviour of the tool under consideration of the maximum loading (worst-case scenario) conditions tested in the field. In the field experiments, average and maximum resultant draft forces were measured as 33,514 N and 51,716 N respectively. The FEA revealed that the maximum deformation value of the tool was 9.768 mm and the maximum stress values impart a change on the most critical structural elements of between 50 and 150 MPa under a worst-case loading scenario. Additionally, a validation study revealed that minimum and maximum relative differences for the equivalent stress values between experimental and simulation results were 5.17 % and 30.19 % respectively. This indicated that the results obtained from both the experimental and simulation are reasonably in union and there were no signs of plastic deformation on the Para-Plow elements (according to the material yield point) under pre-defined loading conditions and a structural optimisation on some of the structural elements may also be possible.

This research provides a useful strategy for informing further research on complicated stress and deformation analyses of related agricultural equipment and machinery through experimental and advanced CAE techniques.

Keywords: Agricultural Machinery, Para-Plow, Design Analysis, Experimental Stress Analysis, Finite Element Analysis

48 1. Introduction

49 As a specific branch of the machinery design and manufacturing industry, agricultural engineering
50 considers the production and maintenance of tractors, agricultural machinery and agricultural
51 implements/tools/equipment. It has gained more attention in recent years since global food/agricultural production
52 has become vitally important in terms of feeding the world population. The current world population of 7.3 billion
53 is estimated to reach 8.5 billion by 2030, 9.7 billion by 2050 and 11.2 billion by 2100 according to the UN DESA
54 report: “World Population Prospects - The 2015 Revision” (UN DESA 2015). There is no doubt that, in order to
55 produce sufficient volumes of food from currently available agricultural land, well-designed machinery and
56 high-tech supported mechanisation for agricultural production is one of the most vital necessities. Most especially,
57 the need for advanced computer aided design (CAD) and engineering (CAE) applications in the manufacturing
58 processes in the agricultural engineering industry have important roles to play (Sha 2008). As such, it is
59 fundamental that the agricultural engineering industry should be equipped with the most appropriate advanced
60 design and manufacturing technologies in order that they can manage to provide sustainable, high-technology,
61 higher precision and increased capacity machinery systems for efficient agricultural production in the finite land
62 available.

63 CAD and CAE, structural optimisation and computer aided manufacturing (CAM) technologies have been
64 used efficiently for product development, design and machinery manufacturing applications in related industries
65 globally for a great number of years. These technologies provide important advantages in end-product time,
66 product quality, manufacturing precision, design costs and the effective organisation of labour force issues in the
67 overall product development and manufacturing processes. However, in many developing countries such as
68 Turkey, most of the agricultural machinery manufacturers are classified as small and medium-sized enterprises
69 (SMEs) that have not yet properly adopted advanced design technologies (Ileri 2018; AEA 2017) where limited
70 research literature exists related to implementation strategies of advanced CAD and CAE applications. Thus, it is
71 important that this research area is given the due consideration it deserves in order to develop robust design
72 strategies, and to produce more efficient and structurally optimised agricultural machinery systems.

73 Soil tillage is one of the most important stages for the cultivation of crops in agricultural production.
74 However, there are a number of problems that affect product yield negatively in seed bed preparation and
75 production of plants in agricultural fields where soil compaction is experienced. In this context, producers use
76 subsoiler and chisel tools in the fields where soil compaction is deemed problematic in agricultural production.
77 These types of tools are classified as deep tillage equipment and require higher power and energy use compared
78 to other tillage tools. Therefore, studies have been carried out for alternative tillage tools which may require less
79 draft force, less fuel consumption and have a higher work efficiency in comparison to subsoiler and chisel tools.
80 As a result of these studies, the Para-Plow tool was developed in the United Kingdom in recent years as an
81 alternative to subsoiler and chisel tools and is also now receiving positive attention in Turkey. Previous studies
82 support that the Para-Plow is a very efficient tillage tool in terms of time and energy saving in soil loosening
83 (Krause *et al.* 1984; Ehlers and Baeumer 1988; Harrison 1988; Peterson *et al.* 1988, Pierce 1992,
84 Parker *et al.* 1989; Sojka *et al.* 1997; Dorado and Fando 2006; Jafari *et al.* 2008; Friday 2008; Solhjoui *et al.* 2014;
85 Askari and Abbaspour-Gilandeh 2019).

86 Although similar research studies regarding strength analysis of agricultural machinery/equipment and
87 tillage tools can be found in recent literature (Topakci *et al.* 2010; Armin *et al.* 2014; Celik *et al.* 2017;
88 Upadhyay *et al.* 2017; Jiang *et al.* 2018; Matache *et al.* 2019; Yurdem *et al.* 2019), detailed research on strength-
89 based design analysis and product development strategy for a Para-Plow tool by means of advanced CAD and
90 CAE applications and the associated field validation and trials have not been undertaken previously. It therefore
91 follows that an algorithmic design analysis study becomes necessary in order to design and manufacture more
92 efficient and optimum machinery systems used in the agricultural fields as nowadays, more complex and large-
93 scale design engineering approaches and machinery applications are being requested by the industry.

94 Considering the limitations in the literature of advanced CAD and CAE applications related to the
95 agricultural engineering field, most especially on advanced design analysis issues for a specific deep tillage tool
96 (Para-Plow), this study aims to develop a CAD/CAE and experimental methods-based design analysis application
97 algorithm and to conduct a strength-based design analysis case study on a Para-Plow tillage tool. With this aim, as
98 detailed in this paper, an application algorithm was developed and put into practice in a step-by-step design
99 analysis of an agricultural tillage tool (Para-Plow) in order to assist researchers and engineers who study the
100 implementation of advanced CAD and CAE technologies within the agricultural design and manufacturing
101 industry. In the study, experimental field tests and advanced CAD and CAE applications were employed. The
102 study revealed useful design analysis outputs which may be used in structural optimisation studies of the
103 Para-Plow.

104

105 **2. Materials and methods**

106 **2.1. Application algorithm**

107 In this research, an application algorithm which can be integrated to structural design analysis studies for
108 applicable agricultural machinery and equipment such as tillage tools was developed and a case study on strength-
109 based design analysis of a Para-Plow tool was conducted. The algorithm was constructed based on experimental
110 field tests, CAD and CAE techniques. The core application sequence of the developed algorithm is shown
111 in Figure 1.

112

113 (Figure 1. Strength-based design analysis application algorithm for agricultural machinery)

114

115 **2.2. The Para-Plow tool**

116 The Para-Plow is a deep tillage tool whose fundamental design specification was prototyped in the UK by
117 a group of agronomists, soil scientists and engineers (Krause *et al.* 1984; Harrison 1988; Friday 2008;
118 Crook 2014). The most specific design feature of the tool is its tines with inclination up to 45°. The purpose of the
119 Para-Plow is to loosen compacted soil layers at depths of 300 to 400 mm and maintain high surface residue levels.
120 Para-Plowing should be effective at loosening soils that become compacted under the moist conditions of irrigation
121 and thereby improve soil conditions for crop growth (Ewen 2015). The main structural elements of the tool are
122 made from structural steel-based materials. Additionally, heat treatment is applied to the tine tips (plowshare).

123 In the case study detailed in this paper, a Para-Plow tool with two tines which was manufactured by a company in
124 Turkey was considered and specifically focused on a structural design analysis of the tool in order to understand
125 the stress distribution on the tool elements and the total deformation behaviour under predefined test conditions.
126 Key aspects of the technical and dimensional specifications of the Para-Plow tool considered in this research are
127 given in **Figure 2**.

128

129 **(Figure 2. Key aspects of the technical and dimensional specifications of the Para-Plow tool)**

130

131 **2.3. Physical field experiments**

132 Physical experiments/field tests were carried out in order to measure the draft force and experimental stress
133 magnitudes on specific locations of the tool under operational working conditions, which are related to the
134 deformation behaviour experienced by the tool. In the field experiments, draft force and strain-gauge
135 method-based stress measurements were conducted simultaneously. One of the most critical points in
136 determination of strength-based design features of the machinery systems is consideration of the worst-case
137 operating conditions and defining the range of the design variables accordingly, as the worst-case operating
138 condition parameters may become the final design parameters. The measurements in the field experiments were
139 realised in two stages. Firstly, the tool was operated in the nominal tillage depth (350~400 mm); secondly, the
140 tillage depth was increased up to 25 % (to 500 mm) as the worst-case operating condition. This depth is also the
141 greatest depth at which Para-Plow tines can work. Experimental data obtained from the field tests were used in the
142 simulation studies in order to set up and validate the simulation results in addition to evaluation of the tool's
143 physical deformation behaviour.

144 Field tests were carried out at the agricultural research field of Akdeniz University (Aksu-Antalya, Turkey).
145 The experiments were set up on 3 ha (200 m x 150 m) area. The area was divided into parts with 50 m divisions
146 by signposts through the tillage direction **(Figure 3)**. Dominant soil content in the field was clay. Additionally,
147 some of the soil properties such as penetration resistance, moisture content and bulk density were also measured
148 at the test field in order to fully ascertain the soil conditions during the tillage operation. Soil properties were
149 measured at 10 different locations within the testing area. The soil penetration resistance was measured through a
150 hand penetrometer (Eijkelkamp Sti Boka - max. measurement depth: 800 mm; cone angle: 30°; penetrating speed
151 of the cone: 30 mm s⁻¹) in accordance with **ASAE Standard EP542 (2002)**. Average values of the soil penetration
152 resistance and related soil properties are given in **Figure 3** against soil depth. The data measured indicated that
153 maximum soil penetration resistance (Ci) was 3.59 MPa at the working depth between 400 mm and 500 mm which
154 would also be the maximum loading case during tillage for the tool used.

155

156 **(Figure 3. Soil properties of the test field and testing scenario schematic)**

157

158 Draft force measurements were conducted through a computer aided data acquisition system with bi-axial
159 load-pin sensors. The system includes three bi-axial (horizontal and vertical) load-pins

160 (BATAROW-MB397-75-A), 8-channel, 48-bit data acquisition module (ME-Meßsysteme GmbH-GSV-8), data
161 recording and monitoring computer, electronic fasteners and data cables (Batarow 2019). The loading capacity of
162 each load-pin was 75,000 N and the data sampling rate was 10 Hz during draft force measurement. Additionally,
163 a special load-pin connector apparatus design was realised for attachment of the load-pins between the Para-Plow
164 tool and the tractor hitch points. The draft force measurement system, its components and tractor attachment are
165 shown in Figure 4.

166

167 (Figure 4. Components of the draft force measurement system and its tractor attachment)

168

169 A strain-gauge (SG) based strain measurement method was employed for the experimental stress analysis
170 part of the field tests. Measured experimental strain data were converted to equivalent stress data according to the
171 relative engineering strain-stress conversion equations. Five SG rosettes were utilised in total which were placed
172 onto the main frame and the tines of the Para-Plow tool. These measurement locations were selected considering
173 the regions that could provide sufficient information about the deformation of the Para-Plow during tillage. During
174 the strain measurement, HBM K-RY81-6 series three elements ($0^\circ/45^\circ/90^\circ$) 120 ohm rectangular SG rosettes, two
175 modules of 8-channel, 24-bit HBM-QuantumX MX840A data acquisition modules, a data monitoring and
176 recording computer, electronic fasteners and data cables were utilised. The data processing software of CATMAN
177 was the 'on-the-go' monitoring interface during the tests (HBM 2011 a, b). Simultaneous draft force and strain
178 measurements were realised during pre-defined field test operations. 10 Hz data sampling rate was set up in order
179 to record precise and synchronised data between draft force and strain measurements. The strain measurement
180 system, its components and strain-gauge locations are shown in Figure 5.

181

182 (Figure 5. Components of the Strain-Gauge (SG) measurement system and SG locations on the Para-Plow)

183

184 For the first stage of the field experiments, tillage was carried out at a nominal working depth
185 (350~400 mm), with average tractor speed of 4.5 km h⁻¹. The Para-Plow cultivated soil at a tillage distance of
186 900 m (effective cultivated area: 675 m²). During the tests, draft force and strain measurements were recorded
187 without pauses, including field turns, thus, the tool was physically tested in the field at a total tillage distance of
188 18 units (900 m) under nominal operating conditions.

189 One of the factors affecting the traction power during tillage is the speed of the tractor. However, in the
190 tests carried out at a working depth of 500 mm during the second stage of the field experiments, it was observed
191 that the tractor was excessively loaded with the nominal tillage working speed of 4.5 km h⁻¹, the wheel skidding
192 rate was higher than 40 % and it was not possible to work at a constant tillage speed. For this reason, while working
193 at increased tillage depth, the tool was able to be tested at an average tractor speed of 1.2 km h⁻¹. The Para-Plow
194 was operated at a tillage distance of three units at this increased tillage depth (approximately 150 m – effective
195 cultivated area: 112.5 m²). The Para-Plow was overloaded for these increased tillage depth tests in accordance
196 with the aim of the second stage of the field test. In fact, it was observed that it was very difficult to operate

197 efficient tillage with the tool under these conditions. The tool was subjected to overloading other than for the
198 design purpose; control of the movement of the tractor became difficult and it was deemed could have dangerous
199 consequences for the loss of life and property. Hence, this case was approved as the worst-case loading scenario
200 for the Para-Plow tool during tillage. A schematic demonstration of the computer aided data acquisition systems
201 for draft force and strain measurements utilised in the field tests and pictures taken during field tests are shown in
202 **Figure 6**. After completion of the field experiments, draft force and equivalent stress data obtained from the field
203 experiments were recorded, precisely processed and represented numerically with graphical visuals. These visual
204 outputs and the processed test data for draft force against equivalent stress values are given in **Figure 7, Figure 8**
205 and **Table 1** respectively.

206

207 **(Figure 6. Schematic demonstration of the computer aided data acquisition systems and the pictures taken**
208 **during field tests of nominal (tillage depth: 400 mm) and worst-case (tillage depth: 500 mm) tillage operations)**

209

210 **(Figure 7. Field Test Results-01: Draft force and experimental stress values of nominal tillage condition)**

211

212 **(Figure 8. Field Test Results-02: Draft force and experimental stress values of worst-case tillage condition)**

213

214 **(Table 1. Draft force and equivalent (von Mises) stress values extracted from field tests)**

215

216 **2.4. CAD Modelling and finite element analysis**

217 A reverse engineering approach was utilised to create a CAD model of the Para-Plow tool. All geometric
218 features and functional limitations of the tool's elements were taken into consideration and solid models of the
219 elements were created in a SolidWorks (SW) 3D parametric software environment using advanced solid modelling
220 techniques. Thus, visual evaluations for the tool were successfully performed in the digital environment. One of
221 the criteria used in the evaluation of the ability of the CAD models prepared to represent physical structures is the
222 mass criterion. The total mass of the tool was calculated through the material property parameters which were
223 defined in the solid modelling software. The total mass for the Para-Plow CAD assembly was automatically
224 calculated as 610.22 kg by the software. When this value is compared with the tool's catalogue data of total mass
225 (600 kg), it is considered that the CAD modelling operations were correctly conducted and the difference of
226 10.22 kg is an acceptable value relative to the total mass. After the completion of solid modelling and assembly
227 operations, the Para-Plow tool was also evaluated in terms of suitability for manufacturing and physical assembly.
228 In this assessment, the criteria such as the tractor attachment positions of the tool before, during and after tillage,
229 tillage functionality, inter-elements compatibility, collision tests, degrees of freedom of the elements, and the
230 stability during transportation etc. were considered and carefully examined. As a result of all the evaluations
231 carried out, no problematic geometry regarding the Para-Plow CAD assembly was observed, hence the design was
232 approved in order to perform finite element method (FEM) based structural analyses. Some statistical data related
233 to the CAD assembly, visual outputs of the final CAD assembly and its tractor attachment are shown in **Figure 9**.

234

235 (**Figure 9.** Some statistical details and visuals from the Para-Plow CAD Modelling Procedures)

236

237 For the strength analysis studies, in order to evaluate the failure conditions of the structural elements of a
238 product, determination of the failure criterion is an important issue as designers make critical decisions on the final
239 strength-based design of products according to such criterion. In both experimental and FEM based stress analyses
240 of the Para-Plow tool considered in this research, the failure criterion was assumed to be the yield stress point of
241 the material. In order to measure the yield point of materials used in the Para-Plow design, tensile testing was
242 employed. The materials for the test specimens were collected from the manufacturer's stocks which were as
243 assigned for the Para-Plow manufacturing. The specimens were extracted from three different samples of identical
244 metal sheets (thicknesses of 2.5 mm, 6 mm and 8 mm), and three specimens for each thickness, i.e. nine specimens
245 in total were tested. Dog Bone Type 2 specimens were prepared and the tests were carried out according to
246 TS EN ISO 6892-1 through the 100 kN tensile capacity test device of SHIMADZU AG-X. The resultant data
247 obtained from the tensile tests were processed, evaluated and average values were calculated in order to appoint
248 them to the simulation set up respectively. According to this evaluation, the average yield, average ultimate tensile
249 and average fracture stress points were 280.26 MPa, 404.23 MPa and 348.69 MPa respectively. Some of the visual
250 and numerical details related to the tensile testing process and the results are given in **Figure 10.**

251

252 (**Figure10.** Material testing results and determination of failure criteria (material yield point))

253

254 During the field tests, the Para-Plow was subjected to an excessive loading at the tillage depth of 500 mm
255 which was defined as the worst-case loading scenario. Soil reaction forces reached the maximum value at this
256 tillage condition, so the tool was forced to structurally deform more than the deformation magnitude experienced
257 at the nominal tillage condition. The Finite Element Analysis (FEA) was set up in order to simulate the defined
258 worst-case loading condition for the tool. ANSYS Workbench FEM based commercial analysis code was
259 employed for the simulation. The FEA was set up under the assumptions of linear static loading and a linear
260 homogeneous isotropic material model. Bonded and No Separation (sliding) linear contact types for welding
261 locations and assembly surfaces were defined for the model respectively. The finite element (FE) model of the tool
262 was created via meshing functions of the code. In order to obtain satisfactory levels of mesh quality with due
263 consideration for structure size and computing platform capacity, pre-trials were realised and uniform meshing
264 strategy was applied with the meshing parameters of maximum element size (10 mm), defeature size (0.5 mm)
265 and element size growth rate (1.25). Total of 406,152 elements and 924,490 nodes were obtained in the FE Model
266 of the tool. In order to verify the mesh quality of the FE model, a skewness metric was utilised in the code.
267 Skewness is one of the primary quality measures for a mesh structure. Skewness determines how close to ideal a
268 face or cell is. According to the definition of skewness, a value of 0 indicates an equilateral cell (best) and a value
269 of 1 indicates a completely degenerate cell (worst) (ANSYS Doc. 2019). The average skewness metric value
270 obtained was 0.245 which indicated an excellent cell quality for the FE model (**Figure 11**). Properties obtained
271 from material tests were taken into consideration in the FEA. The yield strength measured from the material tests

272 was approximately 280 MPa. This value was defined as the material failure criterion with Von Mises failure
273 theory. In the FEA operations, a structural steel-based material was defined with the material parameters of
274 modulus of elasticity (210 GPa), Poisson's ratio (0.3), and the material density (7850 kg m⁻³). A Dell Precision
275 M4800 series mobile workstation was used as the solving platform (Intel Core i7-4910Q-2.9 GHz, 32 GB RAM,
276 NVIDIA Quadro K2100M-2GB, DDR5). Boundary conditions and details of the FE model are given in [Figure 11](#).

277

278 [\(Figure 11](#), Boundary conditions assumed in the FEA, details and verification (Skewness check) of the FE
279 model)

280

281 After completion of the pre-processor steps such as solid modelling, material definition, boundary
282 conditions and preparation of the FE model, the FEA was run. The FEA solution showed the visual deformation
283 behaviour of the tool and equivalent (Von Mises) stress distributions on the tool elements in detail. According to
284 the results, the maximum deformation (displacement) value was 9.7687 mm for the whole structure. When it is
285 compared with the Para-Plow dimensions, it was interpreted that this deformation magnitude would not be
286 detrimental for an effective tillage operation and could be considered within acceptable design limits under pre-
287 defined loading conditions. In the analysis of the strength limits of the tool, it was investigated whether the material
288 yield strength (280 MPa) was exceeded or not at any point of the whole Para-Plow structure, as the yield point is
289 the critical threshold to failure phenomenon for the materials. Although no abnormality was witnessed on the
290 deformation behaviour of the tool, simulations results highlighted excessively high stress concentrations on some
291 single elements at sharp corners and lineal contact regions. Therefore, the stress analysis results identified for these
292 regions were re-investigated. As a result of these subsequent deeper investigations, it was determined that the stress
293 magnitudes were excessively high and the results were not proportional against the pre-defined loading conditions
294 and displacements calculated. Here, the simulation results were re-checked to determine whether any methodical
295 or numerical errors might be experienced in the FEA of the Para-Plow. In a FEA study set up in order to represent
296 pre-defined real physical conditions, numerical errors may occur during the establishment of the mathematical
297 model (e_1), the mathematical discontinuity (e_2), and the numerical solution processes (e_3) ([Figure 12](#)) ([Salmi 2008](#);
298 [Narasaiah 2008](#); [Pancoast 2009](#)). In addition to these methodical errors that might be experienced during a FEA
299 study, user-based errors can occur during interpretation of the results, so should also be kept under consideration.
300 Most especially, FEA solutions utilised for structural stress analysis, excessive and meaningless stress
301 concentrations on sharp corner and contact locations, which is known as a stress singularity, may be experienced.
302 In order to represent an ideal physical structure in a FEA simulation, the common approach is using a smaller
303 element size at the critical loading locations with sharp corners, constraint points or contact regions in the FE
304 model, however, in the stress singularity cases experienced in a FEA solution, an increase in stress values against
305 constant displacement values at these specific locations are observed ([Andy's Log 2012](#); [Grieve 2006](#)).
306 The singularity can be calculated on a critical element which experiences excessively high stress values at a critical
307 location in a FEA solution. The singularity can be diagnosed if the relative difference between stress values
308 measured at two corner points on an identified single element is greater than 30%. In this scenario, the excessive
309 stress values on related locations can be ignored ([Souza et al. 2011](#)).

310 A stress singularity case in the FEA of the Para-Plow tool was explored in accordance with related scientific
311 literature (Huebner *et al.* 2001; Andy's Log 2012; Coskun and Soyhan 2011, SolidWorks Doc. 2011,
312 Souza *et al.* 2011). The singularity control showed that cases on some elements (specifically on two elements: tine
313 connection plates and a welding point on the main frame) in the FEA of the Para-Plow was diagnosed and these
314 values were ignored in the evaluation of the stress analysis results. Errors in FEA approach, the calculation method
315 for singularity diagnosis and a singularity example experienced in the Para-Plow analysis are given in Figure 12.

316 Numerical methods and engineering simulation studies are very useful in visualising more detailed
317 information than experimental and analytical analysis, however some assumptions have to be kept under
318 consideration in the numerical method-based solutions. These assumptions may lead to some of the errors
319 mentioned above. Here the stress analysis results for a Para-Plow were successfully evaluated, singularity-based
320 errors were eliminated and deformation behaviour of the tool was successfully simulated under a defined worst-
321 case loading scenario. Except for singularity points calculated in the FEA results, it was observed that the
322 equivalent stress values on the tool elements were under the limit of the failure criterion. In accordance with the
323 yield point of the material, safety factor distributions on the tool were also calculated. This calculation revealed
324 that there was no plastic deformation evident on the tool elements and the safety factors on the tool elements had
325 a change between 2 (approx.) and 15. The simulation output including deformation, equivalent (Von Mises) stress,
326 safety factor plots and stresses at SG locations are given in Figure 13.

327

328 (Figure 12. General errors in a FEA approach, singularity check and sample singularity calculation from the
329 FEA results of the Para-Plow)

330

331 (Figure 13. Output results of the FEA: Equivalent stress distribution, safety factor distribution and deformation
332 distribution)

333

334 3. Results and discussion

335 Structural design analysis of the Para-Plow tool was successfully carried out by means of experimental and
336 numerical method-based stress analyses. However, a validation study is an important part of an efficient FEA
337 study in order to evaluate and scale reliability and accuracy of the simulation results against real-life physical
338 conditions as the numerical method-based simulations are described as an approximation method for complex
339 engineering problems. In this regard, a validation study was carried out in order to scale the reliability and accuracy
340 of the FEA set up for the Para-Plow. In the validation study, stress analysis results at the SG locations obtained
341 from experimental and simulation studies were compared. Reliability and accuracy of the simulation results were
342 scaled against experimental results by performing calculations for relative differences in percentage at the SG
343 locations. The relative difference in percentage was calculated according to Equation 1 given below (Kurowski
344 and Szabo 1997).

345

346
$$\text{Relative difference in percentage} = \frac{\sigma_{Exp.} - \sigma_{FEA}}{\sigma_{Exp.}} \times 100 \quad (1)$$

347 Here, σ_{Exp} and σ_{FEA} are experimental and the FEM based equivalent (Von Mises) stress analysis results
 348 in MPa calculated at the specific SG locations respectively.

349

350 The validation calculations revealed that relative differences in percentage between experimental and FEA
 351 equivalent stress results at the SG locations were 30.19 % (SG-01), 11.72 % (SG-02), 5.36 % (SG-03),
 352 5.17 % (SG-4) and 7.30 % (SG-05) respectively. The numerical results of the calculations were represented by a
 353 double axis chart as given in **Figure 14**. Research studies in the literature indicate that acceptable relative
 354 differences in percentage between experimental and simulation studies may vary up to 30 % depending on the
 355 complexity of the physical environment to be simulated (Caliskan 2011; Celik *et al.* 2012; Sivaraos *et al.* 2015;
 356 Celik *et al.* 2017; Yurdem *et al.* 2019). For instance, Yurdem *et al.* (2019) reported an experimental (strain-gauge)
 357 and FEM-based structural stress analysis study on a three-bottom moldboard plough. A good correlation between
 358 FEA and the field test and a weight reduction on the tool elements were reported as positive outputs of the research.
 359 The validation error percentage between FEA and the experiments were between 6 % and 29 % (approximately)
 360 against draft force of 20,000 N (tillage depth: 250 mm) in their study. This percentage in the validation study seems
 361 compatible with the values obtained in the Para-Plow study (**Figure 14**). Besides this, there is belief that the
 362 acceptable relative difference rate of a healthy FEA approach should be less than 10 % (Krutz *et al.* 1984;
 363 Sakakibara 2008). However, it should be considered that the differences between experimental and simulation-
 364 based results can vary dependent on analysis type, geometry idealisation level, FE model, boundary conditions set
 365 up in a FEA and unpredictable physical conditions during the experiments. The scale of the absolute numerical
 366 results against the failure criteria should also be kept under consideration. Therefore, the comparative evaluation
 367 of the experimental and FEA results should be carried out taking into account the factors mentioned above.

368 As such, although the relative difference of 30.19 % at the SG-01 location appears greater than may be
 369 expected, the absolute stress values for experimental and FEA results were quite close to each other at this SG
 370 location (8.28 MPa and 10.78 MPa respectively). The absolute difference was 2.50 MPa which may be thought of
 371 as an insignificantly small value against the failure criteria (280 MPa). In this context, it can be confirmed that the
 372 validation study revealed that experimental and simulation results exhibited good correlation within an acceptable
 373 range.

374

375 **(Figure 14. Validation study: Comparison of the experimental and the FEA stress results at SG locations)**

376

377 The equivalent stress distribution on the Para-Plow tool was successfully exhibited through FEA
 378 simulation. The results indicated that the failure threshold (material yield stress point) was not exceeded at any
 379 location on the tool elements except for a couple of singularity points where singularity diagnoses were approved
 380 by related calculations. Except for these singularity locations (which could be ignored), the maximum stress
 381 concentrations which vary by 50 MPa-150 MPa were found at the welding joints on the frame of the tool, as these

382 locations have sharp and thin geometries and it was very logical to expect higher stress values at these locations.
383 Safety factor calculations indicated that the rest of the elements have very high values up to 15 which might be an
384 indicator for a structural optimisation study with the objective of reducing the material weight. Matache *et al*
385 (2019) carried out a FEA on a newly designed and manufactured deep tillage tool (MAS-65). In their study, the
386 maximum structural deformation of the tool was determined as 5.795 mm against draft force magnitude of
387 13,573 N (tillage depth: 450 mm). In the case study detailed in this paper, maximum deformation was calculated
388 as 9.768 mm against draft force magnitude of 51,716 N (tillage depth: 500 mm), so the global deformation
389 magnitude of the Para-Plow may be considered relatively lower than their design in a linear approach, which is an
390 indication of a more durable structure during deep tillage operation.

391 Advanced CAD and CAE simulations supported with physical field tests and related manufacturing
392 applications in the agricultural machinery manufacturing industry are very limited in the area of design of
393 agricultural machinery and related agricultural mechanisation systems, most especially in developing countries. In
394 this research, an application algorithm based on experimental and advanced CAE techniques was developed and a
395 case study for a Para-Plow tillage tool was successfully realised. In the case study, physical tests, CAD and CAE
396 applications were applied step-by-step, numerical and visual results were exhibited and FEA evaluation techniques
397 were discussed, hence, a successful design analysis study in order to generate an optimum design was successfully
398 achieved. The advanced engineering processes described in the case study would be very useful for increasing the
399 product quality, ensuring savings in design, testing and manufacturing times, having efficient work and maximum
400 profits by reducing the material wastage. This case study would also be appropriate as a ‘how-to’ strategy for
401 researchers and engineers in academia and industry. A successful design analysis study for different agricultural
402 machinery and equipment used in tillage, seeding, harvesting and transportation would be realised through the
403 methods, application algorithm and physical and digital test strategies covered by this research. This research also
404 has an active role in order to improve industrial design strategies with well-designed effective products through a
405 university-industry collaboration.

406

407 **4. Conclusions**

408 In this research, the aim was to describe strength-based structural design features which may be used in the
409 structural design studies of a new Para-Plow tool nominated as an effective alternative tool to subsoiler and chisel
410 tools especially in agricultural fields that have experienced soil compaction problems. Within the scope of this
411 research, an application algorithm was developed based on CAD, CAE techniques and experimental methods that
412 can be used in the total design development, improvement and structural optimisation processes of the Para-Plow
413 and similar agricultural machinery, tools and equipment. In this manner, the aim of the research was accomplished
414 and a successful case study was represented.

415 In the case study, physical field tests compatible with CAD, CAE and structural optimisation techniques were
416 performed on the Para-Plow. The results obtained from the physical tests were compared with the results of the
417 simulation and the design validation results were represented. The modelling stage of the case study did not
418 experience any assembly errors or difficulties as advanced CAD modelling techniques were applied and digital
419 models were successfully created. Failure risks on the materials were clearly exhibited through FEA simulations.
420 Additionally, structural optimisation indicators and the feasibility of reducing the material weight and total cost of

421 the tool were discussed. Design validation of the tool was successfully realised through physical field tests and
422 tillage efficiency of the tool was tested. No functional disturbance on the tool during tillage was observed. The
423 FEA was validated by experimental results and showed that they have a good correlation within material limit
424 values. In this research, advanced applications related to CAD and CAE technologies in the agricultural machinery
425 research field have been successfully exemplified.

426 In consideration of small and medium sized enterprises, although advanced engineering applications
427 supported by CAD / CAE are widely used in other machinery design and manufacturing industries, it cannot be
428 said that they are effectively used in the design and manufacturing of agricultural machinery. Hence, use of these
429 types of CAE applications and methodologies in the agricultural machinery industry would be very useful in terms
430 of generating optimum design, incurring less time and cost losses and scientific verification and improving global
431 marketing skills. Thus, it would be possible to contribute to the development of the agricultural machinery design
432 and manufacturing industry.

433

434 **Acknowledgements**

435 This research study was supported financially by The Scientific Research Projects Coordination Unit of
436 Akdeniz University (Turkey) Grant number: FBA-2015-601, 2015. Additionally, the authors wish to acknowledge
437 contribution of Lancaster Product Development Unit (LPDU) at Lancaster University (United Kingdom) in
438 technical evaluation processes employed in this research paper.

439

440 **References**

- 441
- 442 Andy's Log. 2001. Stress Singularities. Online: <http://andreweib.wordpress.com/2010/12/14/stress-singularities/>
443 (Last Accessed: 12.09.2019)
- 444 ANSYS Documentation, 2019, Meshing User's Guide: Skewness. Release 2019 R2, ANSYS Inc., USA.
- 445 Armin, A., Fotouhi, R., Szyszkowski, W. 2014. On the FE modelling of soil-blade interaction in tillage operations,
446 Finite Elements in Analysis and Design, Vol. 92, 1-11
- 447 ASAE Standards, 49th ed. 2002. EP542. Procedures for using and reporting data obtained with the soil cone
448 penetrometer. St. Joseph, Mich.: ASAE.
- 449 Askari, M. and Abbaspour-Gilandeh, Y. 2019. Assessment of adaptive neuro-fuzzy inference system and response
450 surface methodology approaches in draft force prediction of subsoiling tines, Soil & Tillage Research, 194
451 (2019) 104338
- 452 Batarow, 2019, Available URL: <http://www.batarow.com/en/> (Last Accessed: 03.09.2019)
- 453 Çalışkan, K. 2011. Traktör emniyet çerçevesinde dayanım optimizasyonunun laboratuvar test sonuçları ile
454 doğrulanmış sonlu elemanlar yöntemi simülasyonu yardımıyla gerçekleştirilmesi. Doktora Tezi. Ege
455 Üniversitesi, FBE, İzmir, 91 s. (In Turkish)
- 456 Celik, H. K., Caglayan, N., Cinar, R., Ucar, M., Ersoy, H., Rennie. A. 2012. Stress Analysis of a Sample Marine
457 Crane's Boom Under Static Loading Condition. 5th International mechanical engineering forum (IMEF2012),
458 Prague, CzechRep., ISBN 9788021322912. 246-256.
- 459 Celik, H.K., Rennie, A.E.W., Akinci, I. 2017. Design and structural optimisation of a tractor mounted telescopic
460 boom crane. J Braz. Soc. Mech. Sci. Eng. 39:909–924, DOI 10.1007/s40430-016-0558-y.
- 461 Coşkun, G. ve Soyhan, H.S. 2011. Sonlu elemanlar ağ yöntemi yaklaşımına dayalı kenar civarındaki gerilim
462 dağılımlarının tekillikleri. Mühendis ve Makine, 52 (614): 116-125.
- 463 Crook, I.D. 2014. The Howard Para-Plow. Victorian Sales Manager, Crop Protection ICI Australia Operations Pty
464 Ltd. Bayswater, Vic. 3153. Available URL: <http://www.regional.org.au/au/roc/1984/roc198467.htm>
465 (Last Accessed: 02.09.2019)
- 466 Dorado, J. and Lopez-Fando. C. 2006. The effect of tillage system and use of a Paraplow on weed flora in a
467 semiarid soil from central Spain, Weed Research 46, 424–431.
- 468 Ehlers, W. and Baeumer, K. 1988. Effect of the Paraplow on Soil Properties and Plant Performance ISTRO 11th
469 International Congress: Tillage Traffic in Crop Production), Vol. 2, 637-642.
- 470 Ewen, B.M. 2015, Effect of Para-Plowing on Soil Properties and Crop Yield under Irrigated Management. MSc
471 Thesis, Department of Soil Science, University of Saskatchewan, Saskatoon, Saskatchewan, Canada, P75.
- 472 Friday, N.W., Davis H.B., Dey, A.D. 2008. Simon and P. Mc Farlane, Reduced Tillage Systems For Heavy Coastal
473 Clay Soils in The Guyana Sugar Industry, XXIX Conference of West Indies Sugar Technologists, Montego
474 Bay, Jamaica, April 21-25, 2008.
- 475 Grieve, D.J. 2006. Errors Arising in FEA. Online: <http://www.tech.plym.ac.uk/sme/mech335/feaerrors.htm>
- 476 Harrison, P.H. 1988. Soil Reacting Forces for a Bentleg Plow, Transactions of the ASABE. 31 (1): 0047-0051.
477 (DOI: 10.13031/2013.30663)
- 478 HBM 2011a. Datasheet: QuantumX MX840A. Doc. No: B2924-2.0 en. Hottinger Baldwin Messtechnik GmbH,
479 Germany.

480 HBM 2011b. Strain Gages and Accessories. Doc. No: S 1265-1.0 en. Hottinger Baldwin Messtechnik GmbH,
481 Germany, 100 s.

482 Huebner, K.H., Dewhirst, D.L., Smith, D.E., Byrom, T.G. 2001. The Finite Element Method for Engineers. John
483 Wiley & Sons. ISBN: 9780471370789, 744 p.

484 Ileri, M.S. 2018. TARMAKBIR (The Turkish Association of Agricultural Machinery & Equipment
485 Manufacturers) Sector Report 2018 for Turkish Agricultural Machinery Industry (05.02.2018;
486 Revision 22.02.2019)

487 Jafari R., Raoufat M.H., Tavakoli Hashjin T. 2008. Soil-Bin Performance of a Modified Bent Leg Plow, Applied
488 Engineering in Agriculture. 24(3): 301-307. (DOI: 10.13031/2013.24493)

489 Jiang, Q., Xu1, L., Xue, B., Zhang, Z. 2018. Design and analysis of a bionic pull-type subsoiler, Academic journal
490 of manufacturing engineering, vol. 16, (4), 46-53.

491 Krause, R., Lorenz, F., and Hoogmoed, W.B. 1984. Soil Tillage in the Tropics and Subtropics, Eschborn. Published
492 by Deutsche Gesellschaft für Technische Zusammenarbeit (GTZ) GmbH, Germany, p.320.

493 Krutz, G., Thompson, L., Claar, P. 1984. Design of Agricultural Machinery. John Willey & Sons, ISBN:
494 047108672, 473 s.

495 Kurowski, P. and Szabo, B. 1997. How to find errors in finite element models. Machine Design, 9: 93-98

496 Matache, M.G., Remus, M.O., Dragos, N.D., Gheorghe, G V., Cujbescu, D., and Persu, C. 2019. Structural analysis
497 of deep soil loosening machine MAS-65. Les Ulis: EDP Sciences.
498 DOI:<http://dx.doi.org/10.1051/e3sconf/201911203034>

499 Narasaiah, L.G. 2008. Finite Element Analysis. BS Publications. ISBN:9788178001401, 340 p.

500 Pancoast, D. 2009. Solidworks Simulation-2010 Training Manual. Dassault System Solidworks Corporation.
501 Doc. No: PMT1040-ENG. 486 p.

502 Parker, C., J., Carr. M.K.V., Jarvis, N.J., Evans, M.T.B. and Lee, V.H. 1989. Effects of subsoil loosening and
503 irrigation on soil physical properties, root distribution and water uptake of, potatoes (*Solanum tuberosum*). Soil
504 and Tillage Research 13, 267–285.

505 Peterson, A., E., Swan, J.B., Paulson N.H. and Higgs, R.L., 1988. Effect of Modern Tillage Systems On Residue
506 Management For Corn Production. ISTRO 11th International Congress: Tillage Traffic in Crop Production,
507 11-15th july 1988, vol. 2, 809-814.

508 Pierce, F.J., Fortin, M.C. and Staton, M.J. 1992. Immediate and Residual Effects of Zone-Tillage on Soil Physical
509 Properties and Corn Performance. Soil and Tillage Research 24, 149–165.

510 Sakakibara, N. 2008. Finite Element in Fracture Mechanics. Lecture Notes. The University of Texas, Austin, USA.

511 Salmi, S. 2008. Multidisciplinary Design Optimization in an Integrated CAD/FEM Environment. MSc Thesis,
512 Dept. of Mathematical Information Technology, University of Jyväskylä. 70 p.

513 Sha, L. 2008. An application of industrial design in large-scale agricultural machinery. 9th International
514 Conference on Computer-Aided Industrial Design and Conceptual Design, Kunming, China,
515 DOI: 10.1109/CAIDCD.2008.4730688, pp. 823-828.

516 Sivaraos, S.T., Leong, Y., Yusof, C., Tan, F. 2015, An experimental and numerical investigation of tensile
517 properties of stone wool fiber reinforced polymer composites, Adv. Mater. Lett. 6(10), 888-894

518 Sojka, R.E., Horne, D.J., Ross, C.W. and Baker, C.J., 1997. Subsoiling and Surface Tillage Effects on Soil Physical
519 Properties and Forage Oat Stand and Yield. Soil and Tillage Research 40, 125–144.

- 520 Solhjou, A., Fielke, J.M., Desbiolles, J.M.A., and Saunders, C. 2014. Soil translocation by narrow openers with
521 various bent leg geometries. *Biosystems Engineering*, 127, 41e49.
- 522 SolidWorks Documentation. 2011. SolidWorks Simulation. Training Manual Document No: 015600018017-
523 PMT1140-ENG-DRAFT, Dassault Systems SolidWorks Corporation, USA, 486 p.
- 524 Souza, T., S.G., De Souza, M. M., Savoy, J. 2011. Stress Singularity Issue in the Virtual Development of
525 Powertrain Parts. Virtual Powertrain Conference and Expo, 24 25, August 2011. Sao Paulo, Brazil.
- 526 The Agricultural Engineers Association (AEA), 2017, Market Report 2017: Overview of the Agricultural
527 Engineering Market 2017, Available URL: <http://www.aea.uk.com/news-home> (Last Accessed: 02.03.2019)
- 528 Topakci, M., Celik, H.K.; Canakci, M., Rennie, A.E.W., Akinci, I., Karayel, D. 2010. Deep tillage tool
529 optimization by means of finite element method: Case study for a subsoiler tine, *Journal of Food, Agriculture
530 & Environment* Vol.8 (2): 531-536.
- 531 UN DESA, 2015. World population prospects-the 2015 revision: Key findings and advance tables. Dept. of
532 Economic and Social Affairs-Population Division, United Nations, Doc. No. ESA/P/WP.241, New York, USA.
- 533 Upadhyay, G., Raheman, H., Rasool, S. 2017. Three Dimensional Modelling and Stress Analysis of a Powered
534 Single Acting Disc Harrow Using FEA, *Current Agriculture Research Journal*, Vol. 05 (2), 203-219.
- 535 Yurdem, H., Degirmencioglu, A., Cakir, E., Gulsoylu, E. 2019. Measurement of strains induced on a three-bottom
536 moldboard plough under load and comparisons with finite element simulations, *Measurement*, Vol.136, 594-
537 602
- 538
- 539

540 **Figure Captions**

- 541 **Figure 1.** Strength-based design analysis application algorithm for an appropriate agricultural machinery
- 542 **Figure 2.** Key aspects of the technical and dimensional specifications of the Para-Plow tool
- 543 **Figure 3.** Soil properties of the test field and testing scenario scheme
- 544 **Figure 4.** Components of the draft force measurement system and its tractor attachment
- 545 **Figure 5.** Components of the Strain-Gauge (SG) measurement system and SG locations on the Para-Plow
- 546 **Figure 6.** Schematic demonstration of the computer aided data acquisition systems and the pictures taken during
547 field tests of nominal (tillage dept: 400 mm) and worst-case (tillage dept: 500 mm) tillage operations
- 548 **Figure 7.** Field Test Results-01: Draft force and experimental stress values of nominal tillage condition
- 549 **Figure 8.** Field Test Results-02: Draft force and experimental stress values of worst-case tillage condition
- 550 **Figure 9.** Some statistical details and visuals from the Para-Plow CAD Modelling Procedures
- 551 **Figure10.** Material testing results and determination of failure criteria (material yield point)
- 552 **Figure 11.** Boundary conditions assumed in the FEA, details and verification (Skewness check) of the FE model
- 553 **Figure 12.** General errors in a FEA approach, singularity check and sample singularity calculation from the FEA
554 results of the Para-Plow
- 555 **Figure 13.** Output results of the FEA: Equivalent stress distribution, safety factor distribution and deformation
556 distribution
- 557 **Figure 14.** Validation study: Comparison of the experimental and the FEA stress results at SG locations

558

559

560

561 **Table Captions**

- 562 **Table 1.** Draft force and equivalent (von Mises) stress values extracted from field tests

563

564
 565
 566
 567
 568
 569
 570
 571
 572
 573
 574
 575
 576
 577
 578

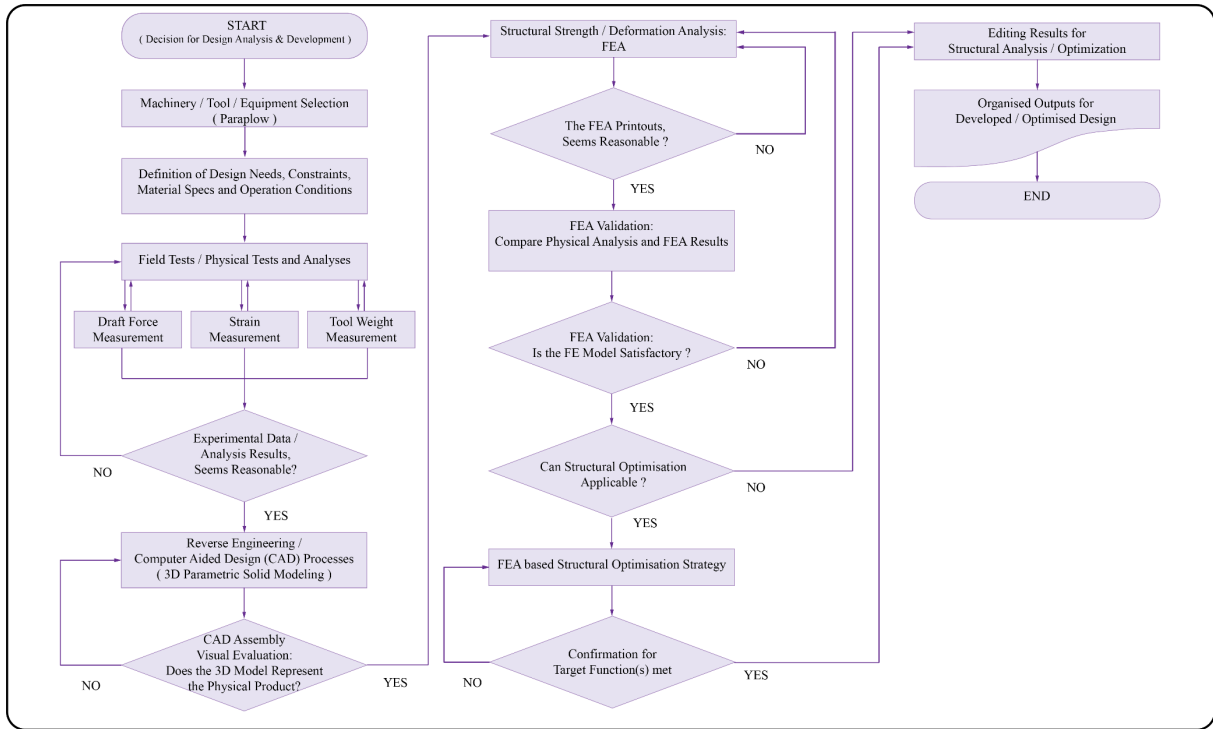
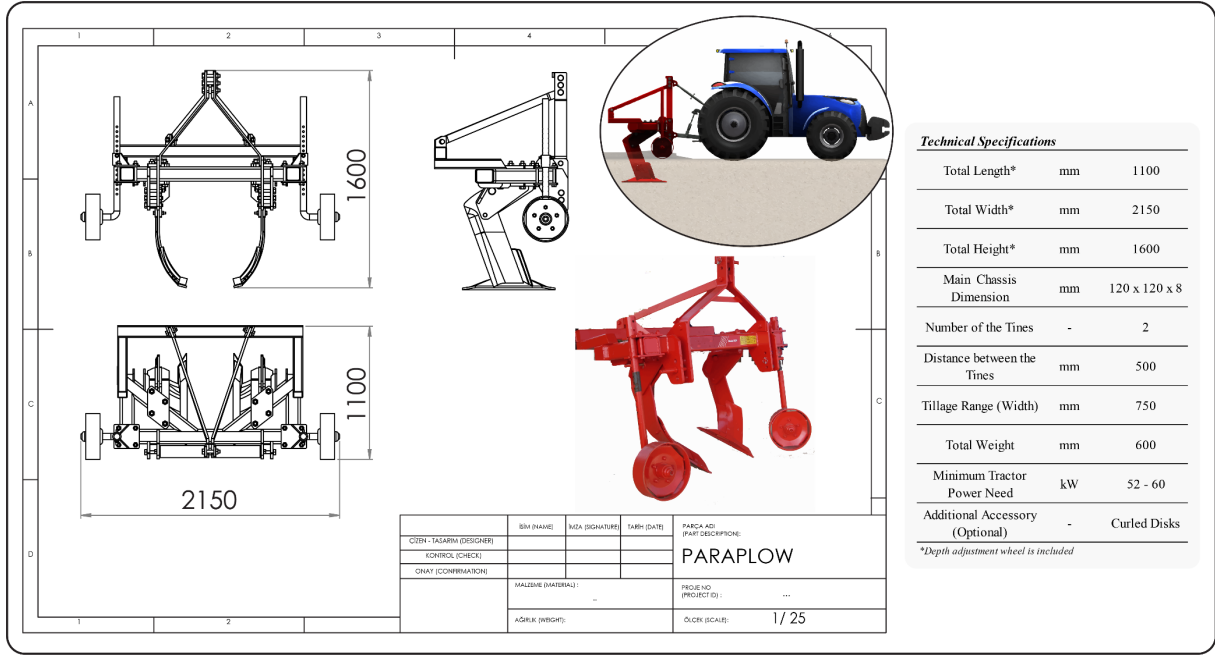


Figure 1. Strength-based design analysis application algorithm for an appropriate agricultural machinery

579
580
581
582
583
584
585
586
587
588
589



590
591
592

Figure 2. Key aspects of the technical and dimensional specifications of the Para-Plow tool

593
 594
 595
 596
 597
 598
 599
 600
 601
 602
 603
 604
 605
 606
 607
 608
 609

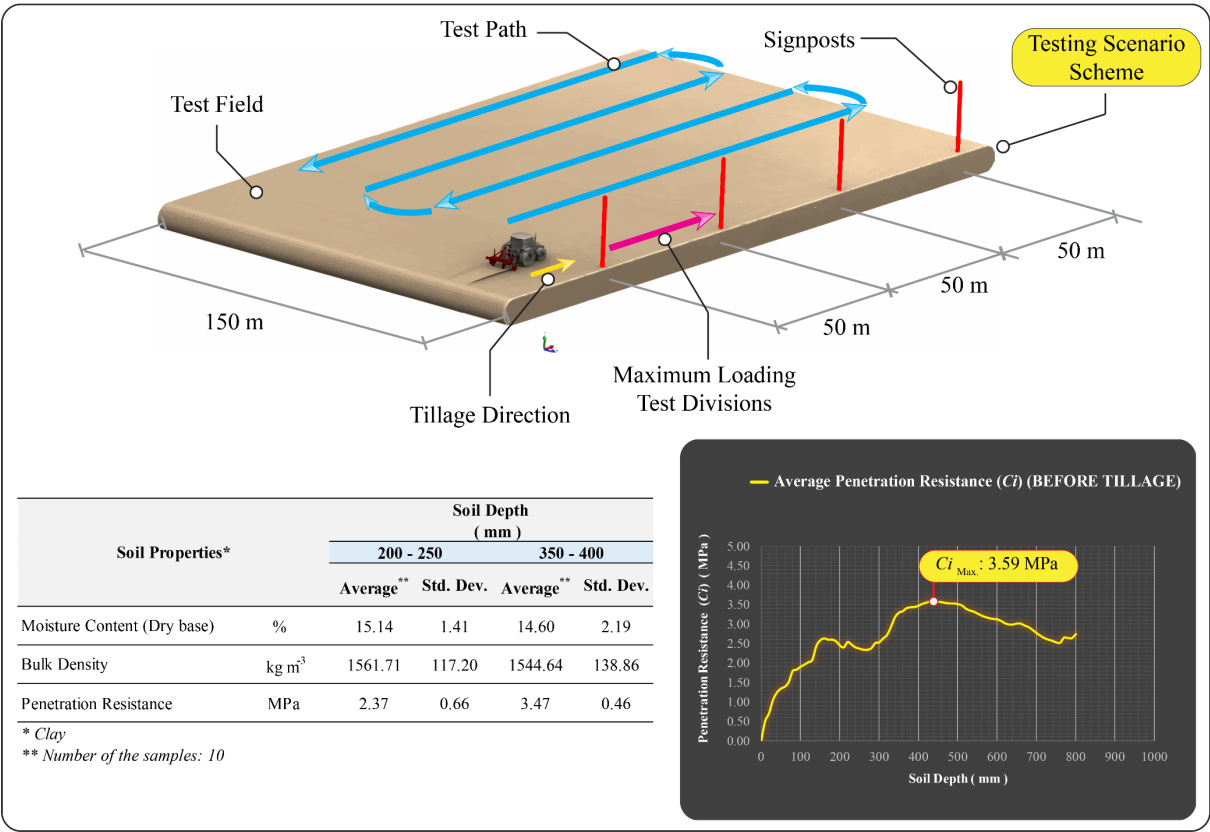


Figure 3. Soil properties of the test field and testing scenario scheme

610
611
612
613
614
615
616
617
618
619
620
621
622
623
624
625
626
627
628

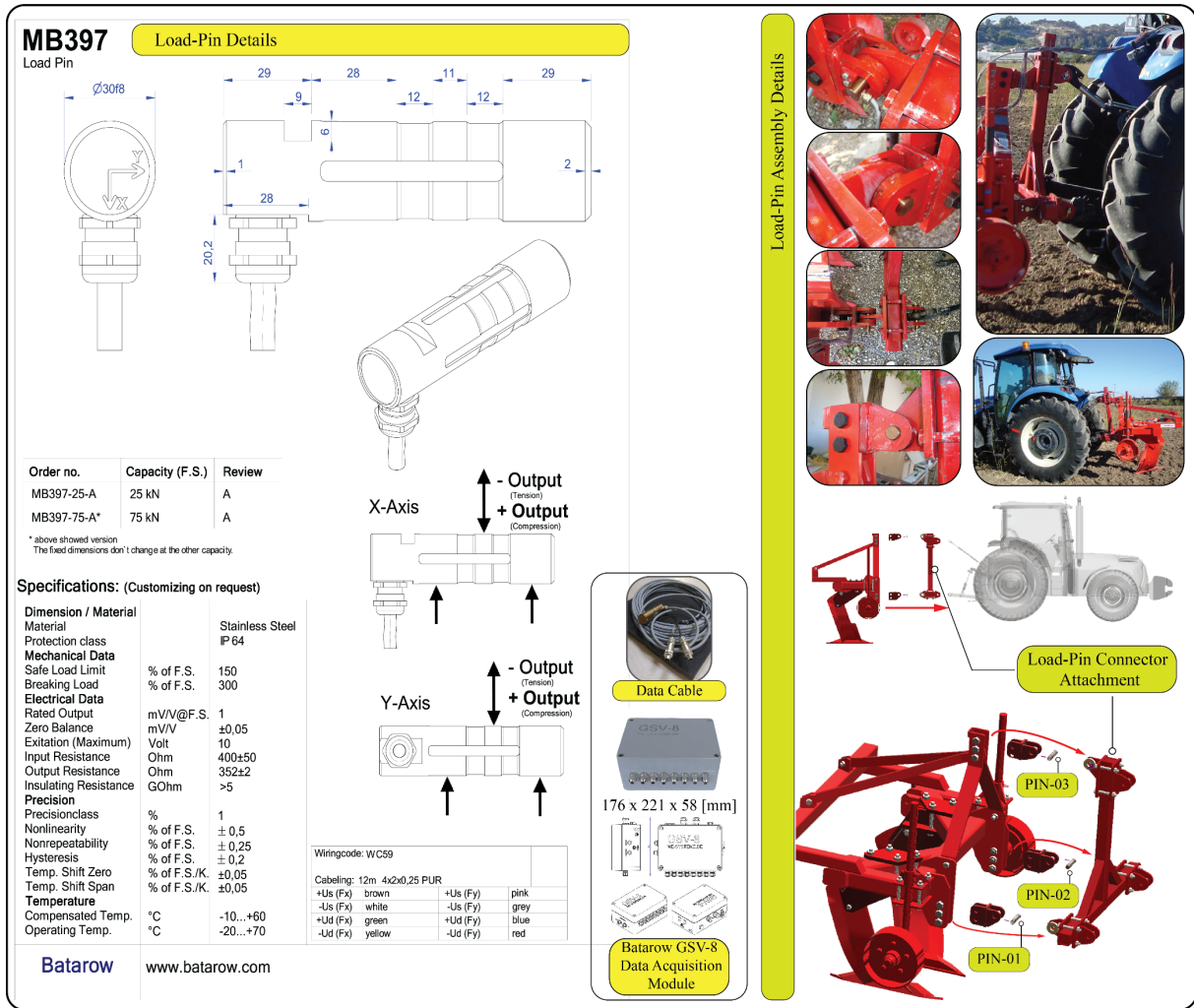


Figure 4. Components of the draft force measurement system and its tractor attachment

629
630
631
632
633
634
635
636
637
638
639
640
641
642
643

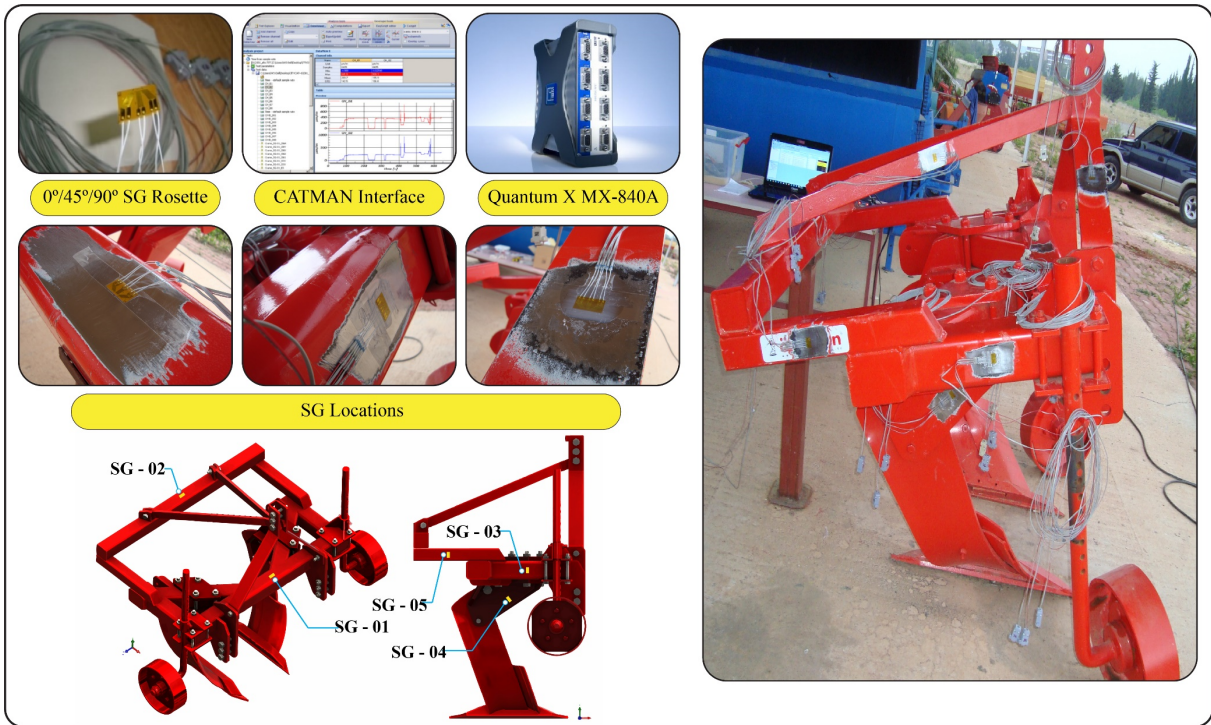


Figure 5. Components of the Strain-Gauge (SG) measurement system and SG locations on the Para-Plow

644
645
646
647
648
649
650
651
652
653
654
655
656
657
658
659
660
661
662
663
664
665

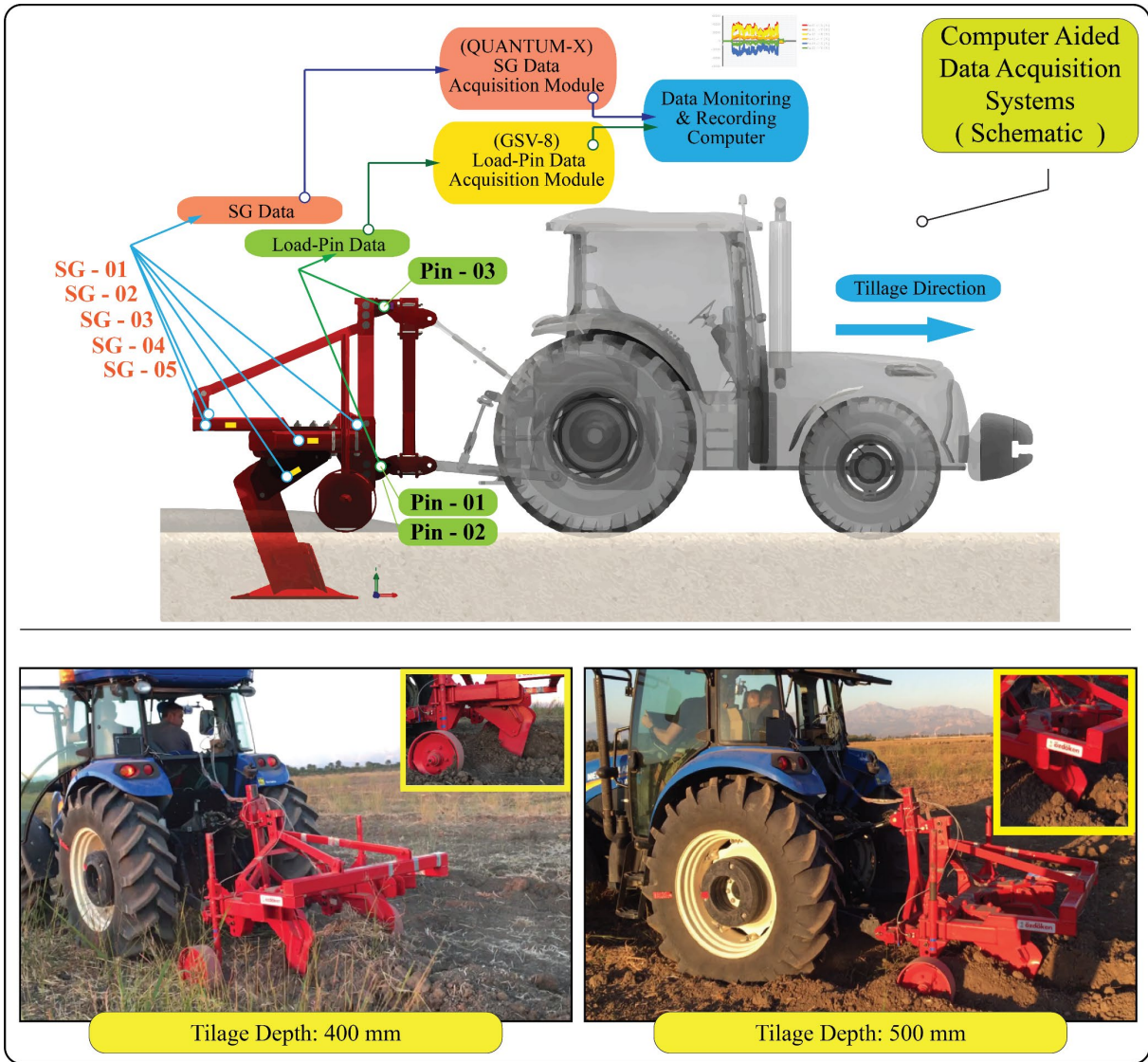


Figure 6. Schematic demonstration of the computer aided data acquisition systems and the pictures taken during field tests of nominal (tillage dept: 400 mm) and worst-case (tillage dept: 500 mm) tillage operations

666
667
668
669
670
671
672
673
674
675
676
677
678
679
680
681
682
683
684
685
686
687
688
689
690
691
692
693
694
695

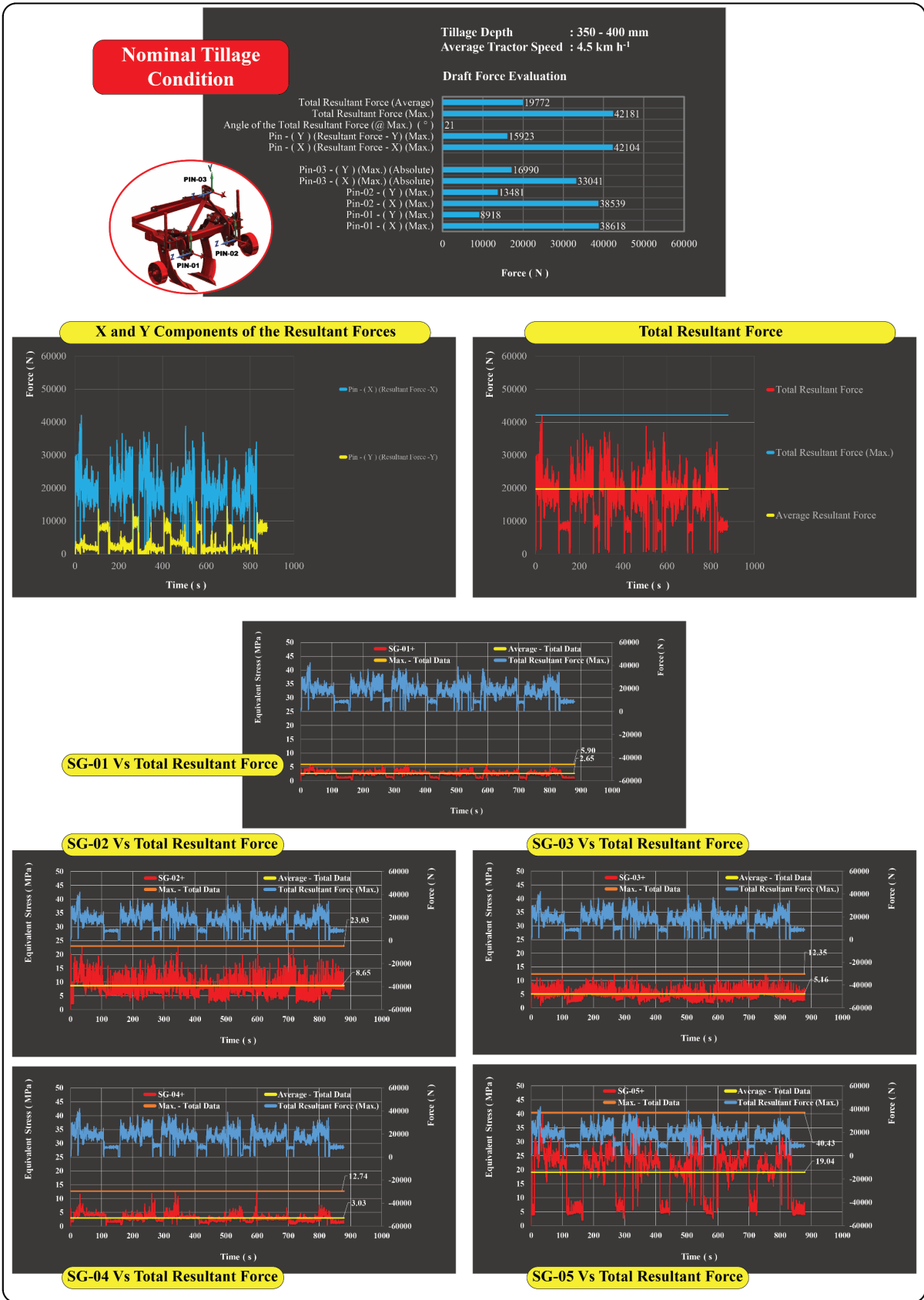


Figure 7. Field Test Results-01: Draft force and experimental stress values of nominal tillage condition

696
 697
 698
 699
 700
 701
 702
 703
 704
 705
 706
 707
 708
 709
 710
 711
 712
 713
 714
 715
 716
 717
 718
 719
 720
 721
 722
 723
 724
 725

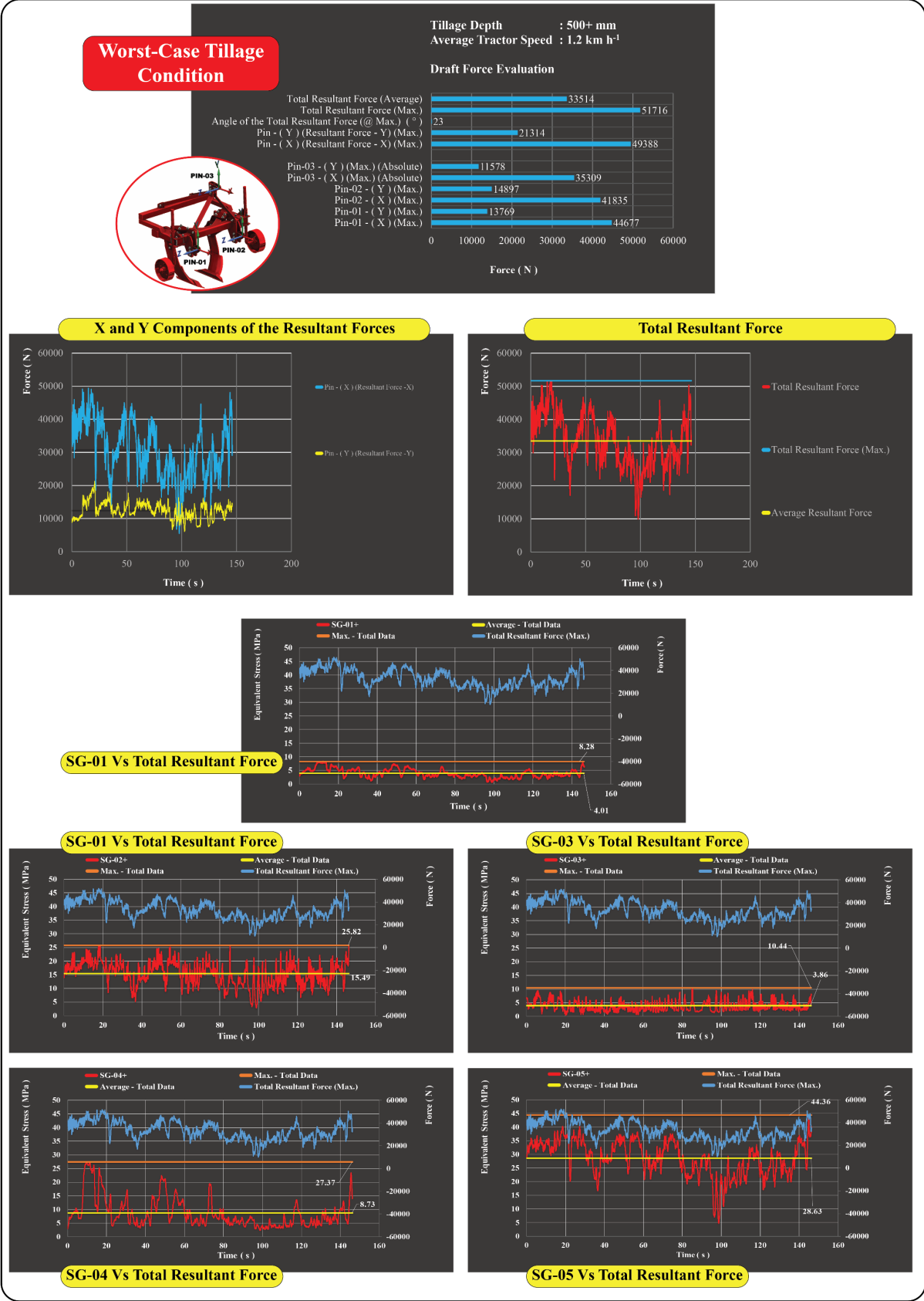


Figure 8. Field Test Results-02: Draft force and experimental stress values of worst-case tillage condition

726
727
728
729
730
731
732
733
734
735
736
737
738
739
740

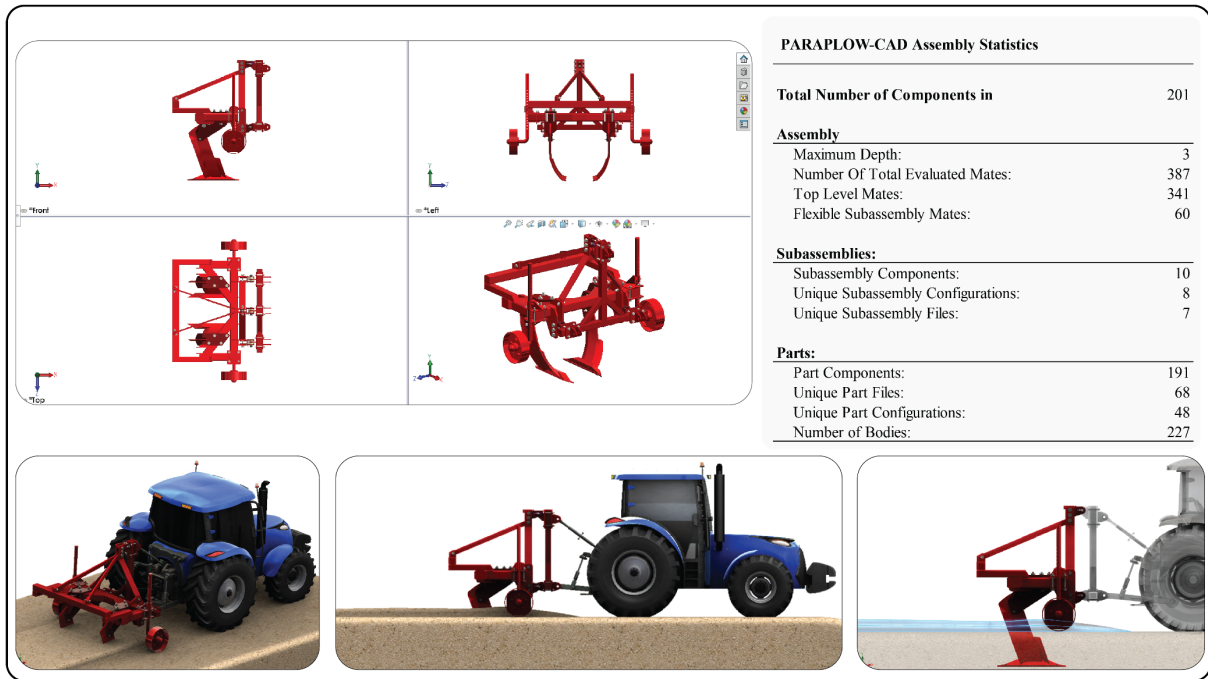


Figure 9. Some statistical details and visuals from the Para-Plow CAD modelling procedures

741
742
743
744
745
746
747
748
749
750
751
752
753
754

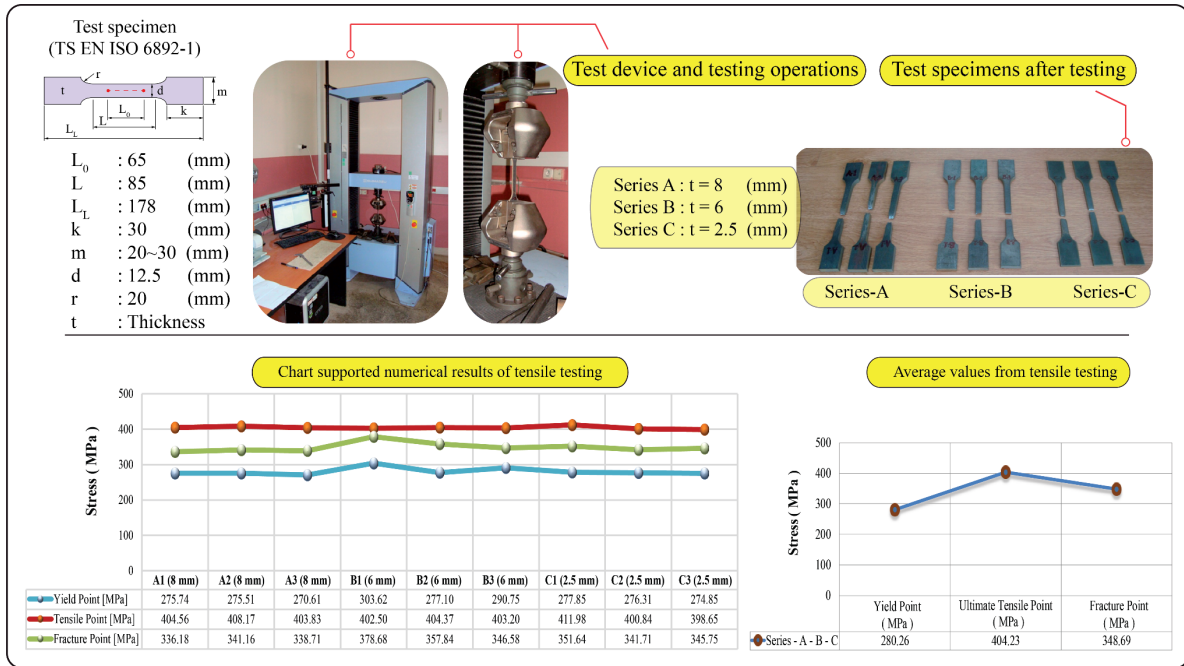


Figure10. Material testing results and determination of failure criteria (material yield point)

755
756
757
758
759
760
761
762
763
764
765
766
767
768

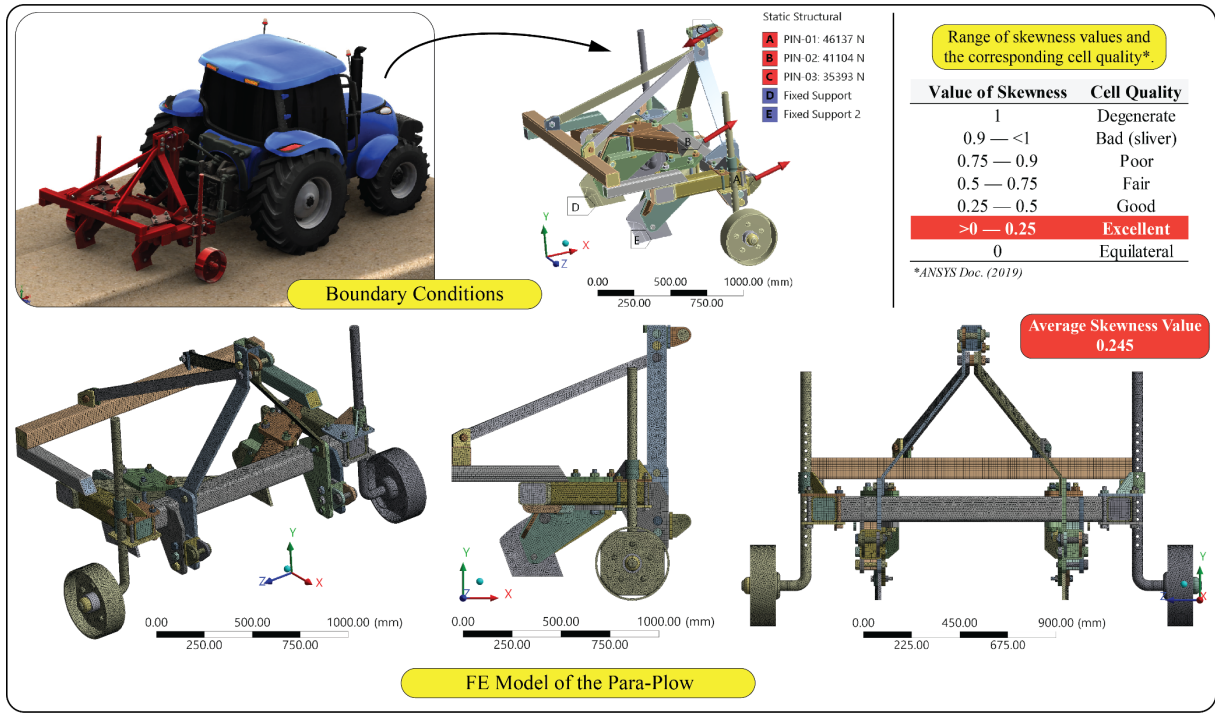
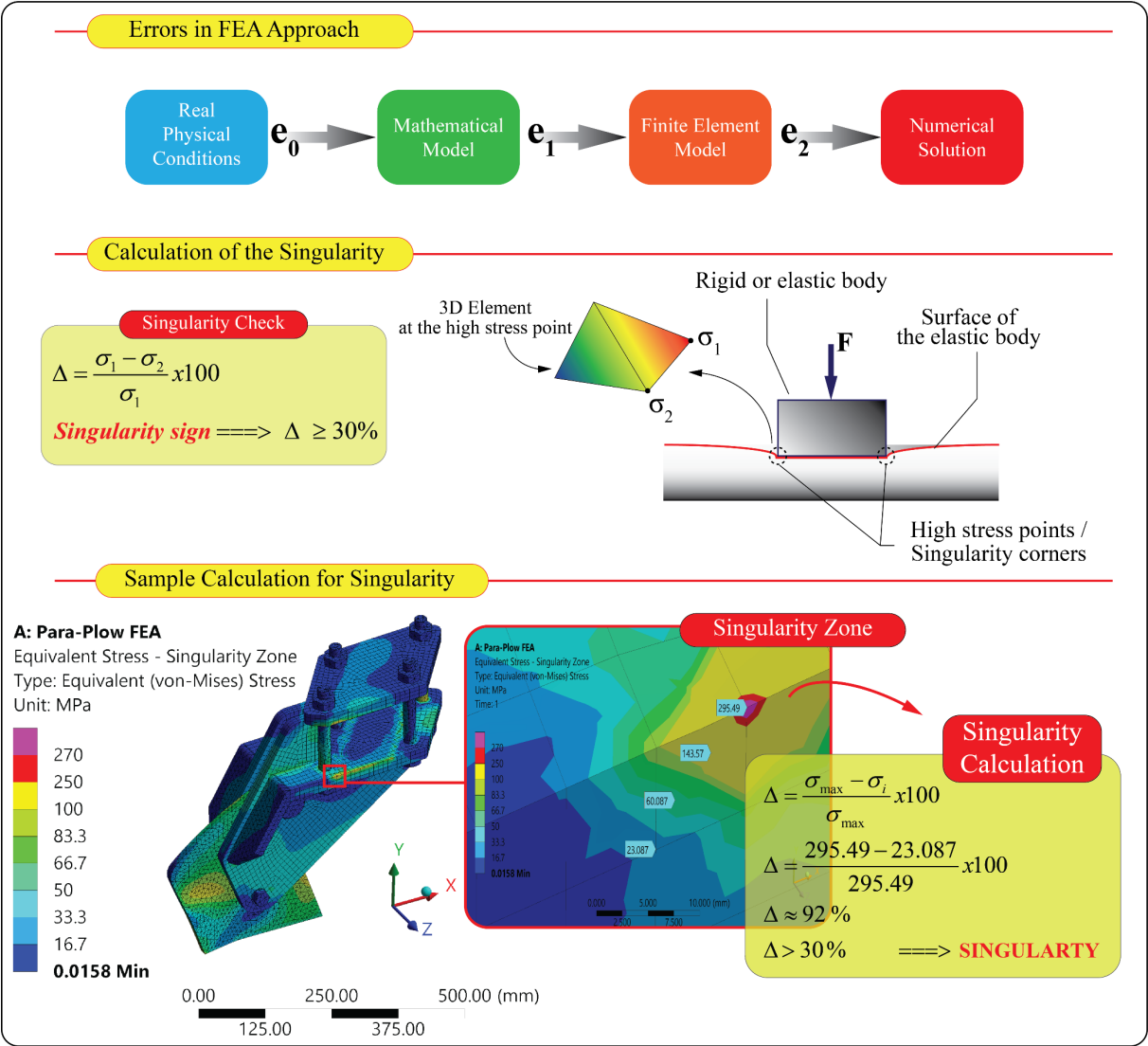


Figure 11. Boundary conditions assumed in the FEA, details and verification (Skewness check) of the FE model



787

788 **Figure 12.** General errors in a FEA approach, singularity check and sample singularity calculation from the FEA

789 results of the Para-Plow

790

791

792
793
794
795
796
797
798
799
800
801
802
803
804
805
806
807
808
809
810
811
812
813
814
815
816
817
818

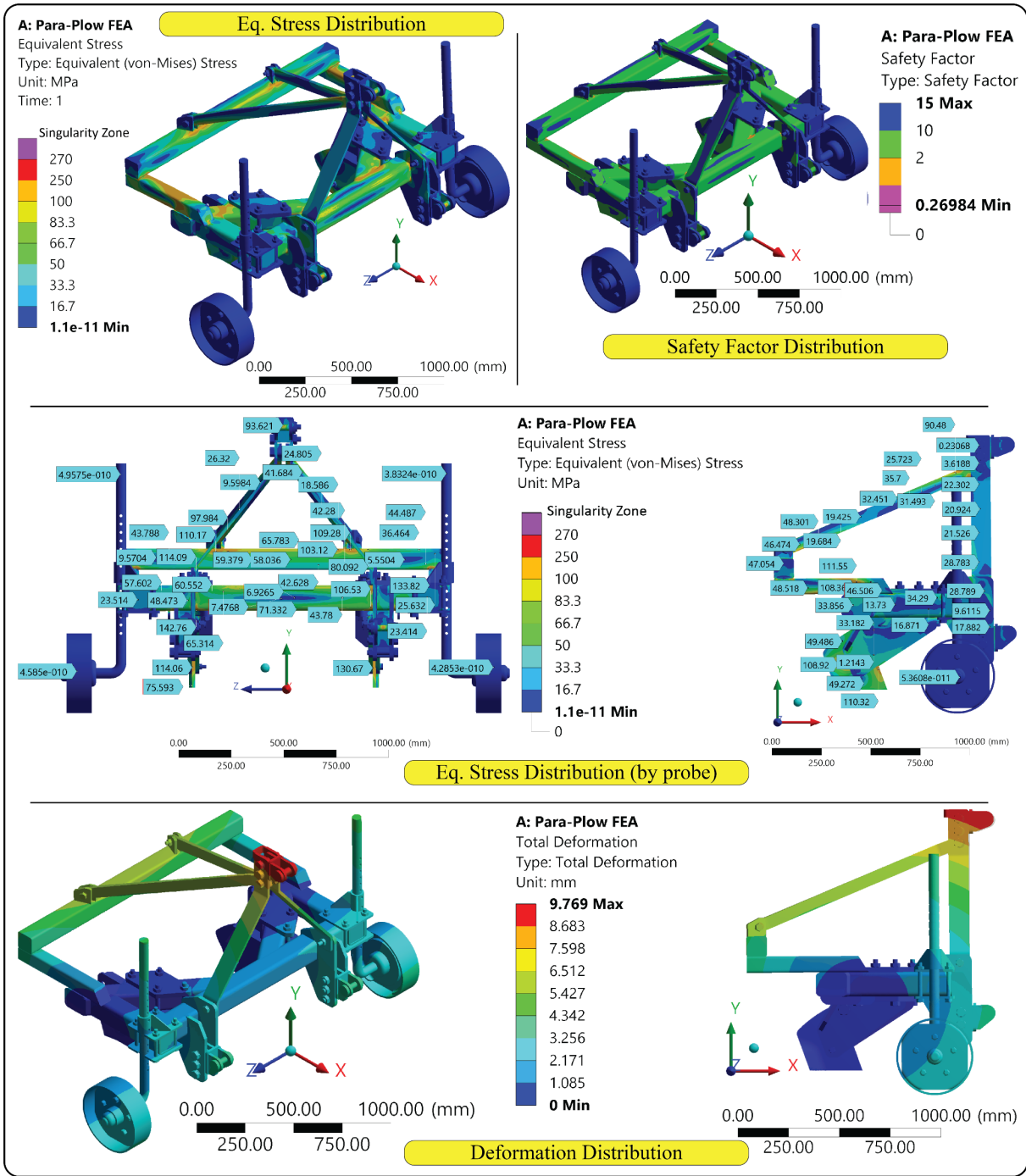


Figure 13. Output results of the FEA: Equivalent stress distribution, safety factor distribution and deformation distribution

819
820
821
822
823
824
825
826
827
828
829
830
831
832
833
834
835
836
837
838
839
840

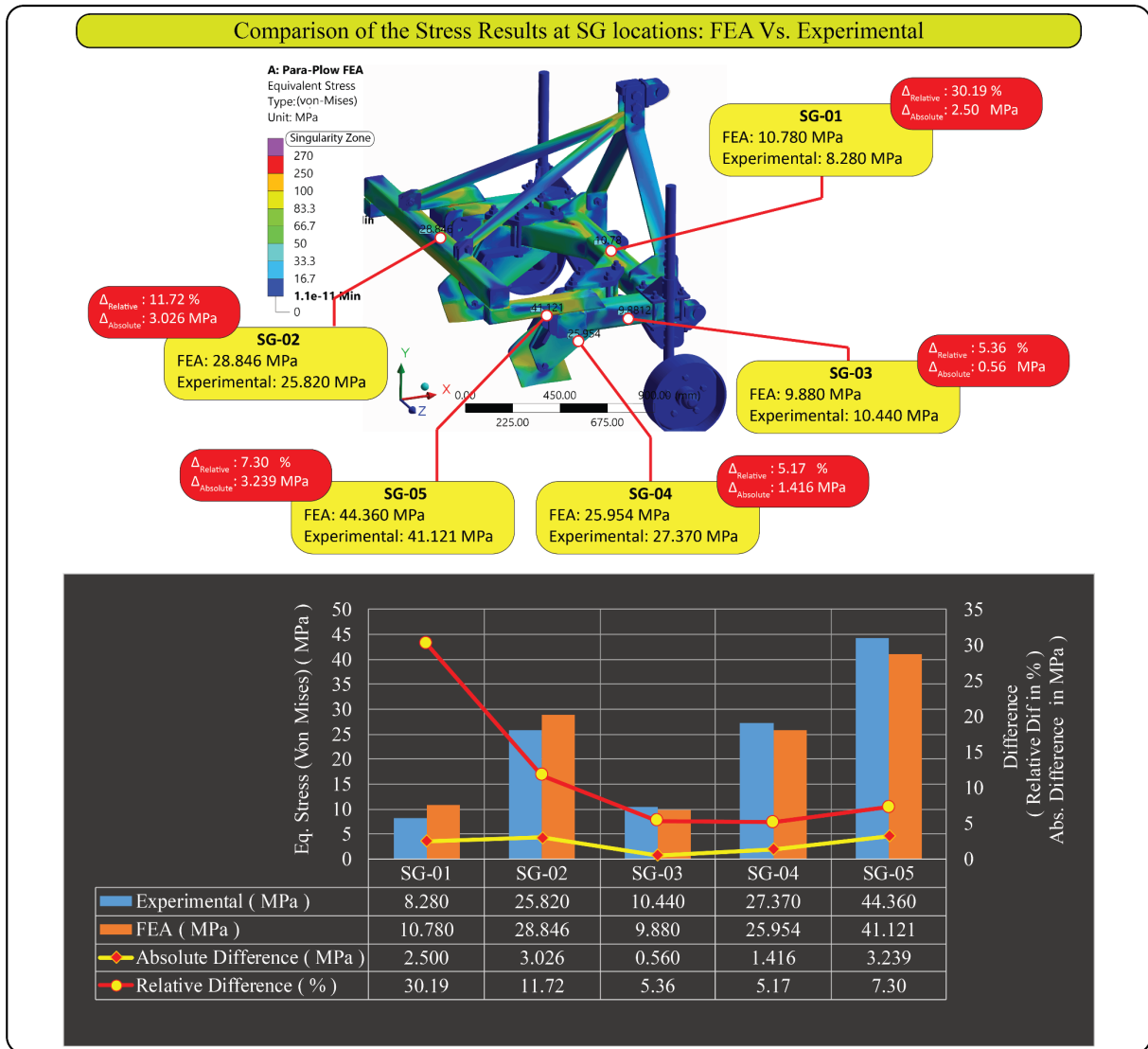


Figure 14. Validation study: Comparison of the experimental and the FEA stress results at SG locations

841

842

Table 1. Draft force and equivalent (von Mises) stress values extracted from field tests

843

844

845

846

847

848

849

850

851

Field Test Conditions	Tillage Depth (mm)	Tractor Speed (Average) (km h ⁻¹)	Tractor Wheel Skidding (Average) (%)	Draft Force		Equivalent (Von Mises) Stress at SG Locations*									
				(Resultant Force)		SG-01		SG-02		SG-03		SG-04		SG-05	
				Max. (N)	Average (N)	Max. (MPa)	Average (MPa)	Max. (MPa)	Average (MPa)	Max. (MPa)	Average (MPa)	Max. (MPa)	Average (MPa)	Max. (MPa)	Average (MPa)
Stage #1: Nominal Tillage Condition**	400	5.0	12	42181	19772	5.91	2.65	23.05	8.65	12.35	5.16	12.74	3.03	40.43	19.84
Stage #2: Worst-Case Tillage Condition	500	1.2	40	51716	33514	8.28	4.00	25.82	15.49	10.44	3.86	27.37	8.73	44.36	28.63

* SG: Strain Gauge

** Operated tillage area: 675 (m²)